Preparation of $LiFePO_4$ Using Chitosan and its Cathodic Properties for Rechargeable Li-ion Batteries

Kyong-Soo Hong, Seong Mi Yu, Myoung Gyu Ha, Chang Won Ahn, Tae Eun Hong, Jong Sung Jin, Hyun Gyu Kim, Euh Duck Jeong,[*] Yang-Soo Kim,[†] Hae-Jin Kim,[‡] Chil-Hoon Doh,[§] Ho-Soon Yang,[#] and Hee Jung[P]

High-Technology Components & Materials Research Center, Korea Basic Science Institute, Pusan 618-230, Korea
[*]E-mail: edjeong@kbsi.re.kr
[†]Suncheon Branch, Korea Basic Science Institute, Suncheon 540-742, Korea
[‡]Energy Nano Materials Team, Korea Basic Science Institute, Daejeon 350-333, Korea
[§]Korea Electrotechnology Research Institute, Changwon 641-120, Korea
[#]Department of Physics, Pusan National University, Pusan 609-735, Korea
[P]Department of Computer Science, Gyeongsang National University, Jinju 660-701, Korea
Received September 2, 2008, Accepted June 9, 2009

The $LiFePO_4$ powder was synthesized by using the solid state reaction method with $Fe(C_2O_4)\cdot 2H_2O$, $(NH_4)_2HPO_4$, Li_2CO_3, and chitosan as a carbon precursor material for a cathode of a lithium-ion battery. The chitosan added $LiFePO_4$ powder was calcined at 350 °C for 5 hours and then 800 °C for 12 hours for the calcination. Then we calcined again at 800 °C for 12 hours. We characterized the synthesized compounds via the crystallinity, the valence states of iron ions, and their shapes using TGA, XRD, SEM, TEM, and XPS. We found that the synthesized powders were carbon-coated using TEM images and the iron ion is substituted from 3+ to 2+ through XPS measurements. We observed voltage characteristics and initial charge-discharge characteristics according to the C rate in $LiFePO_4$ batteries. The obtained initial specific capacity of the chitosan added $LiFePO_4$ powder is 110 mAh/g, which is much larger than that of $LiFePO_4$ only powder.

Key Words: Carbon coating, Chitosan, $LiFePO_4$, Lithium ion batteries

Introduction

The lithium-ion battery has received much attention due to its high voltages which lie in the range of 3.0 ~ 4.5 V. Until recently, the transition metal oxides such as $LiCoO_2$,[1] $LiNiO_2$,[2] and $LiMn_2O_4$[3] are examined as cathode electrodes. Lithium metal phosphates $LiMPO_4$ (M = Mn, Fe, Co, and Ni) attracted lots of attention because of their promising applications as cathode materials for large batteries because of their low cost in rechargeable lithium-ion batteries.[4-6] Among these materials, lithium iron phosphate ($LiFePO_4$) is one of the most interesting materials to fabricate cheaper and safer lithium-ion batteries.[7] $LiFePO_4$ cathode materials have a large theoretical capacity up to 170 mAh/g and high stability during lithium extraction, and are environmentally safe, inexpensive and naturally abundant[6] that could have a major impact in electrochemical energy storage. For $LiFePO_4$, the discharge potential is about 3.4 V *vs.* lithium and no obvious capacity fading was observed even after several hundred cycles. However, $LiFePO_4$ has a poor electric conductivity. If a high current density is applied across the $LiFePO_4$ electrode, the capacity decreases abruptly, this influences its applications significantly. Since the discovery of the electrochemical properties in $LiFePO_4$, extensive efforts have been made to improve the performance of $LiFePO_4$ cathode materials, including addition of conductive Cu/Ag powders and carbon black powders, super-valence cation doping, carbon coating, and synthesis of nanocrystalline grains.[6-9]

In search for improved materials for electrodes, it has been recognized that NaSICON (a family of Na super-ionic conductors) or olivine (magnesium iron silicate type) oxyanion scaffolded structures offer interesting possibilities.[10,11] In order to enhance the electric conductivity, carbon containing $LiFePO_4$ composite seems to be a very promising candidate to overcome the capacity because the well-dispersed carbons provide a pathway for electron transport.[12,13]

Since this material has a very low conductivity at room temperature, it is possible to achieve the theoretical capacity only at a very low current density[14] or at elevated temperatures[15] due to the low lithium diffusion at the interface. Carbon coated $LiFePO_4$ has been prepared using several methods.[16-20] A carbon coating significantly improves the electrochemical performance of this material; sucrose was proposed[16] as a carbon precursor, and it was used on the initial hydrothermal samples.[16] Added carbon increases the electronic contact between the active materials and the electronic conductor, and controls the particle size.[21]

We have tried several methods in order to improve the electric capacity of $LiFePO_4$. For examples, we added organic materials such as humic acid[22] and chitosan, as well as metal elements by using the sol-gel method.[23] In this article, we describe the obtained characteristics when chitosan is added. We synthesized the chitosan added $LiFePO_4$ powders by using the solid state reaction method and checked the crystallinity. We confirmed the valence states of iron ions, and their shapes for the carbon coated $LiFePO_4$. To elucidate the characteristics of the carbon coated $LiFePO_4$ significantly; powders were investigated by using TGA, XRD, SEM, TEM, and XPS. For the electrochemical properties, the electrodes were analyzed using charge-discharge experiment and compared pure $LiFePO_4$ and carbon coated $LiFePO_4$.

Experimental Details

The $LiFePO_4$ materials were synthesized by using the solid state reaction method. The starting materials were iron(II) oxalate dihydrate [$Fe(C_2O_4)\cdot 2H_2O$, Aldrich, 99.99%], ammonium hydrogen phosphate [$(NH_4)_2HPO_4$, Aldrich, 99.99%], and lithium carbonate (Li_2CO_3, Aldrich, 99.95%). The carbon coated $LiFePO_4$ precursor was prepared from the above mixture by adding chitosan (Aldrich) gel in acetic acid. The $LiFePO_4$ precursor was calcined at 350 °C for 5 hours and then 800 °C for 12 hours under reduced atmosphere (Ar/H_2 = 90/10) to reduce the oxidation of iron ions for the first calcination. The material was cooled to room temperature, and the powder was grinded by ball mill system. Then we calcined again at 800 °C under reduced atmosphere (Ar/H_2 = 90/10) for 12 hours. The chitosan added $LiFePO_4$ was calcined twice as described in $LiFePO_4$ only case. Then the chitosan added $LiFePO_4$ was ball milled for 24 hours and calcined again at 350 °C for 5 hours and 600 °C for 12 hours.

The thermal stability of both materials was analyzed by using thermo gravimetric analyzer (TGA, TA Instruments DSC 2920) with the heating rate of 5 °C/min from room temperature to 900 °C. The synthesized materials were characterized by using the conventional X-ray diffractometer (XRD, Rigaku D-2400), X-ray photoelectron spectrometer (XPS, Escalab 250), scanning electron microscope (SEM, Hitachi S-4200), and transmission electron microscope (TEM, JEM 2011).

For the preparation of $LiFePO_4$ cathodes, the synthesized $LiFePO_4$ powders, acetylene black as a conductive material, and *N*-methyl-2-pyrrolidone (NMP) solution containing poly (vinylidene difluoride) (PVDF, Aldrich, average MW: 534,000) as a binder were used. The supporting electrolytes were a propylene carbonate (PC, Mitsubishi Petrochemical Co. battery grade), ethylene carbonate (EC, Mitsubishi Petrochemical Co. battery grade), diethyl carbonate (DEC, Mitsubishi Petrochemical Co. battery grade) and ethyl methyl carbonate (EMC, Mitsubishi Petrochemical Co. battery grade) solution [PC/EC/DEC/EMC, 1:1:1:1 with the volume ratio] containing 1.12 M $LiPF_6$ (Aldrich). For the electrochemical measurement, we prepared $LiFePO_4$ electrodes by mixing 85 wt% bare $LiFePO_4$ and chitosan added $LiFePO_4$, 8 wt% conducting compound as a conductive agent, and 7 wt% PVDF binder to a NMP solution. The kneaded slurry in an adequate viscosity was coated on an aluminum foil. The prepared electrodes were dried at 100 °C in a vacuum oven for 24 hours. Coin-type cell composed of bare $LiFePO_4$ cathode, lithium metal ribbon anode, polyethylene (PE) separator were used in a supporting electrolyte. The charge/discharge experiment was carried out galvanostatically using battery testing instrument (TOSCAT-3000U, Toyo).

Results and Discussion

The thermal analysis gives the optimum calcination temperatures required to prepare the $LiFePO_4$ powders for the decomposition pattern of $LiFePO_4$ precursors. Figure 1 shows TGA curves for (a) $LiFePO_4$ precursor (the solid line) of $Fe(C_2O_4)\cdot 2H_2O$, $(NH_4)_2HPO_4$ and Li_2CO_3 as the starting materials and (b) the chitosan added $LiFePO_4$ precursor (the dotted line). Since significant changes are observed around 350 °C and 800 °C as indicated two vertical arrows in Figure, we chose these two points as the calcination temperatures of the $LiFePO_4$ precursors. The chitosan added $LiFePO_4$ shows weaker weight loss than $LiFePO_4$ precursor below 300 °C. Thus the chitosan added $LiFePO_4$ looks more endothermic below 300 °C region compared with $LiFePO_4$ precursor, which means that the thermal stability is more enhanced due to the added chitosan.

Figure 2 shows XRD patterns of (a) $LiFePO_4$ powder after the second calcination and (b) the chitosan added $LiFePO_4$ powder after the third calcination. Olivine type $LiFePO_4$ phase was observed in $LiFePO_4$ only case after the second calcinations. For the chitosan added $LiFePO_4$ after ball mill process, the XRD peak intensities slightly decreased (not shown). We calcined again to remove acid precipitates during ball mill process and got the patterns as shown in Figure 2(b). There are additional peaks around 40° and 47° (indicated by two vertical arrows) in Figure 2(b). These are due to the remained impurities

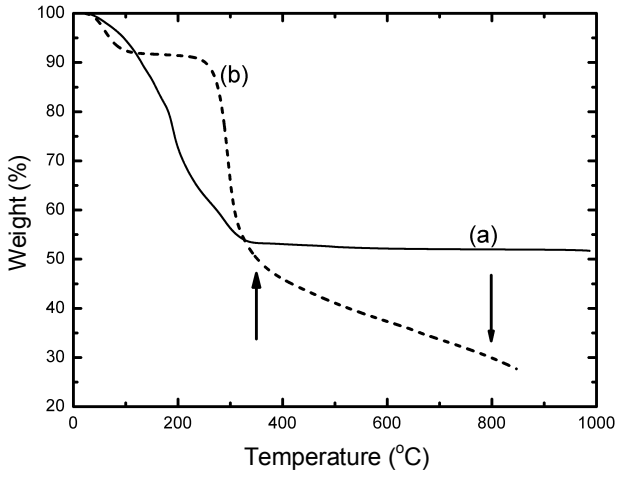

Figure 1. TGA curves of the (a) $LiFePO_4$ precursor (the solid line) and (b) the chitosan added $LiFePO_4$ powders (the dotted line).

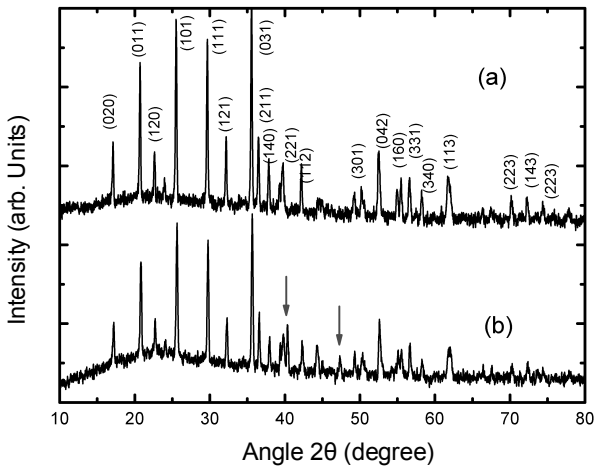

Figure 2. XRD patterns of (a) $LiFePO_4$ powder and (b) the chitosan added $LiFePO_4$ powder. The upper spectra were shifted vertically for clarity.

in the synthesized samples according to the JCPDS files. No significant variation in the grain size was observed in each calcination process.

Figure 3 shows SEM images of (a) $LiFePO_4$ powder after the second calcination and (b) the chitosan added $LiFePO_4$ powder after the third calcination. All powders show uniform structures with similar grain sizes in each case, *i.e.*, before and after adding chitosan. According to the morphology shown in the images, we can find that the influences caused by adding chitosan and the longer calcination clearly.

In order to check the carbon coatings in synthesized powders, we carried out the TEM measurements. Figure 4 shows high-resolution TEM images of the synthesized $LiFePO_4$ powder after the second calcination (left) and the chitosan added $LiFePO_4$ powder after the third calcination (right). When we compare the two images, it is clear that carbon is deposited on the surface of the chitosan added $LiFePO_4$ powder in a form of a nanometer-thick layer of carbon. The thickness of carbon layer is measured to be about 4.1 nm in most of the synthesized powders. We think that this carbon layer gives good electric conductivity of the synthesized material as shown later in this article.

When the precipitates are burned in the air-limited atmosphere such as argon atmosphere in our calcination condition, the oxygen is consumed in the furnace and carbons from the precipitates would remain. These residual carbons are oxidized to CO or CO_2 by taking oxygen. In order to see the oxidation

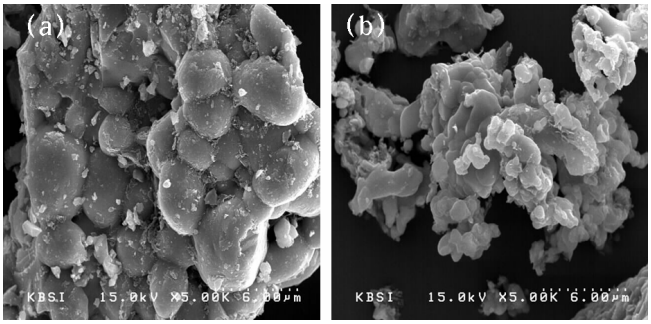

Figure 3. SEM images of (a) $LiFePO_4$ powder after the second calcination and (b) the chitosan added $LiFePO_4$ powder after the third calcination.

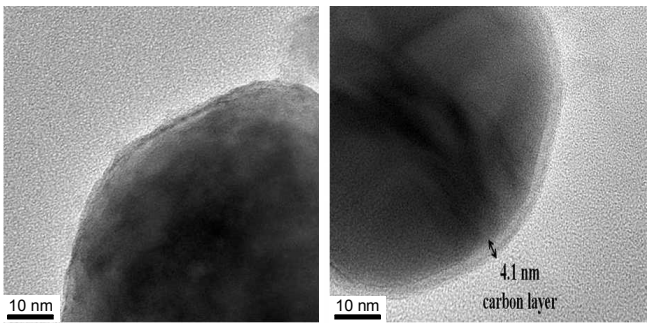

Figure 4. TEM images of the synthesized $LiFePO_4$ powder after the second calcination (left) and the chitosan added $LiFePO_4$ powder after the third calcination (right). The nano-sized carbon layer in chitosan added $LiFePO_4$ powder is clearly observed.

status of carbon and the valence state of iron, we took XPS spectra in all powders. Figure 5 shows wide scan XPS spectra for (a) $LiFePO_4$ powder after the second calcination and (b) the chitosan added $LiFePO_4$ powder after the third calcination. All elements such as Li, P, C, O, and Fe are observed.

The carbon intensities increased a lot when chitosan is added as shown in Figure 5 (The vertical scale of chitosan added $LiFePO_4$ powder is about 12 times stronger than $LiFePO_4$ powder.). Since XPS spectra were taken in vacuum without etching the surface of the samples, the carbon peak in $LiFePO_4$ powder (upper spectra) is considered due to the residual carbon from the atmosphere or the precipitates in synthesis process. In order to see the oxidation and valence states of the iron, we took narrow scan spectra.

Figure 6 shows narrow scan XPS spectra of iron 2*p* state in synthesized $LiFePO_4$ powders. The upper one represents the $LiFePO_4$ powder after the second calcination and the lower one represents the chitosan added $LiFePO_4$ powder after the

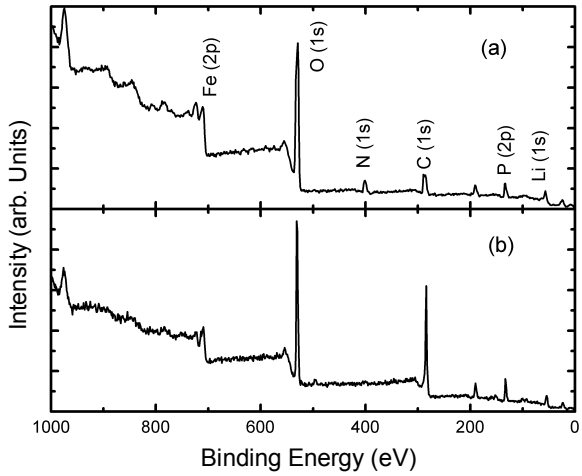

Figure 5. Wide scan XPS spectra for (a) $LiFePO_4$ powder after the second calcination and (b) the chitosan added $LiFePO_4$ powder after the third calcination.

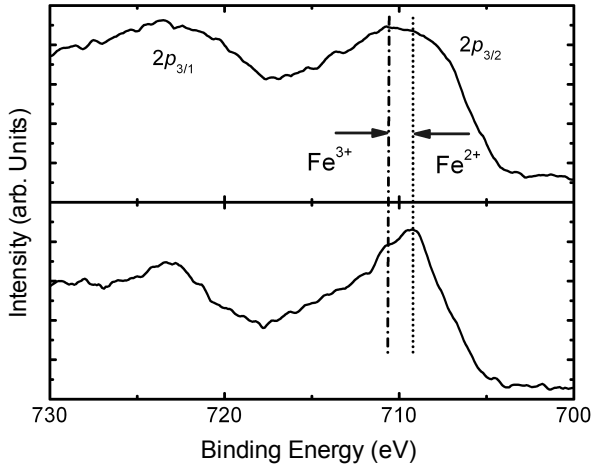

Figure 6. Narrow scan XPS spectra of iron 2*p* in $LiFePO_4$ powders. The upper spectrum represents $LiFePO_4$ powder after the second calcination and the lower spectrum represents the chitosan added $LiFePO_4$ powder after the third calcinations.

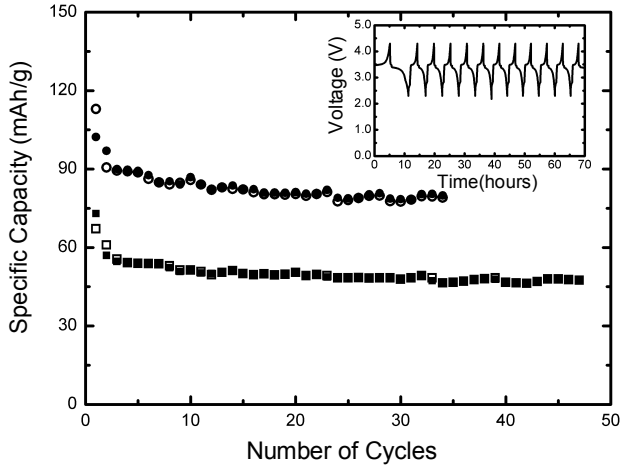

Figure 7. The specific capacity upon discharge rate of 0.2 C with the number of cycles. The squares and circles represent $LiFePO_4$ powder after the second calcination and the chitosan added $LiFePO_4$ powder after the third calcination, respectively. Open and solid points represent charging and discharging processes, respectively. The inset shows the charge-discharge cycles of the $LiFePO_4$ electrodes. The potential range was between 2.5 V and 4.3 V.

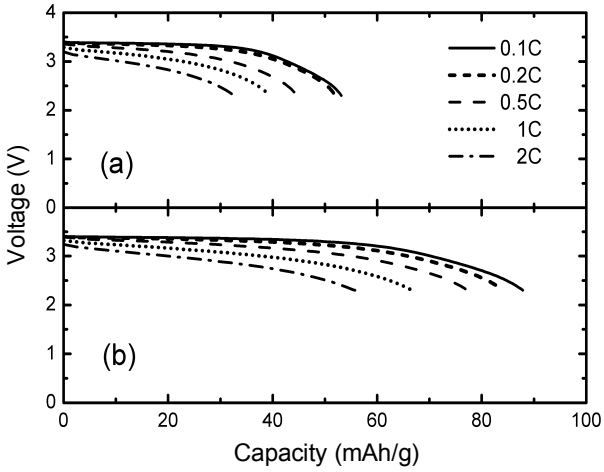

Figure 8. The discharge voltage profiles for the electrodes as a function of the specific capacity for (a) $LiFePO_4$ powder and (b) the chitosan added $LiFePO_4$ powder. In both cases, the charge rate was 0.2 C and discharge rates were different.

third calcination. With the number of calcination times, the iron $2p_{3/2}$ binding energy shifts to lower side. We can think that there is a reaction between $LiFePO_4$ powder and the added chitosan, which means that we obtained $LiFePO_4$ powder with different conditions. The shift of the iron $2p_{3/2}$ binding energy is related to the difference in the oxidation state of iron ions. The shift range of the synthesized powders agrees with the binding energy of the oxidation state of Fe^{2+}.[24] We synthesized $LiFePO_4$ powders in air-limited atmosphere. In this case, burning out the emulsion-precipitates gives rise to the reduction of divalent ions.[25] Since there is no other secondary phase in XRD patterns as shown in Figure 2, most of the iron ions were reduced to Fe^{2+} after the third calcination at 600 °C. Figure 6 implies that the synthesized chitosan added $LiFePO_4$ powder shows an olivine-type $LiFePO_4$ phase with no impurities because the residual carbon contributes to the reduction atmosphere during calcination which is sufficient to reduce Fe^{3+} to Fe^{2+}.[19]

Since there is no other secondary phase except impurities as shown in XRD patterns shown Figure 2, most of the iron ions were reduced to Fe^{2+} after the third calcination at 600 °C. The shift range of the samples agrees with the binding energy of the oxidation state of Fe^{2+}.[24]

As shown in Figure 6, the valence states of iron shifted from 3+ to 2+ with calcination times. Hence the more Fe^{2+} exists in $LiFePO_4$, the more lithium ion can deintercalate from the host and more lithium ion will intercalate into the guest, resulting in higher capacity.[26] In other words, more calcination results in the formation of more Fe^{2+}.

The electrochemical properties of all synthesized powders were analyzed using constant current discharge-charge experiment. Figure 7 shows the charge-discharge profiles obtained at a 0.2 C rate for the $LiFePO_4$ powder after the second calcination and the chitosan added $LiFePO_4$ powder after the third calcination. The potential range was between 4.3 V and 2.5 V. The specific capacity of $LiFePO_4$ powder is slightly decreasing with the number of cycles, but that of the chitosan added $LiFePO_4$ powder is slightly increasing with the number of cycles; from cycle No. 7 to No. 10. As a whole, the capacity shows a decrease. However in both cases, the obtained specific capacities for charge and discharge processes are almost constant with the number of cycles for all compounds. The obtained specific capacity of the chitosan added $LiFePO_4$ powder is larger than that of $LiFePO_4$ only powder, but they are still lower than the theoretical value 170 mAh/g.

We think that this behavior can be controlled by optimizing the electrolyte system and the fabrication technique condition for lithium battery test cell. We can think that the carbon coating improves the cyclability of the cathode materials and adding chitosan can upgrade the electrochemical performance for rechargeable batteries. The charge-discharge cycles of the $LiFePO_4$ electrodes were shown as an inset in the Figure 7.

Figure 8 shows the voltage profiles of the $LiFePO_4$ electrodes as a function of the specific capacity. The charge rate of the electrodes was 0.2 C in all cases in order to assure identical initial conditions. The chitosan added $LiFePO_4$ powders show larger specific capacity compared with those of $LiFePO_4$ powder for the same conditions. The electrode was discharged galvanostatically under different rates from 0.1 C to 2 C. The cut-off voltage was about 2.3 V in all cases. At lower discharge rates, the voltage profiles were kept almost constant during the following intercalation step. For the lowest discharge rate 0.1 C, the electrode was able to deliver a specific capacity of almost 90 mAh/g; which corresponds to the discharge time of about 11.3 hours for the chitosan added $LiFePO_4$ powders. By increasing the discharge rates, we observed a decrease of the average discharge voltages and an increase of the electrode voltage drops.

From the above analysis, we can say that it is possible to synthesize carbon-coated $LiFePO_4$ powder by mixing chitosan by using the solid state reaction method, and the chitosan added $LiFePO_4$ powder increased the electrochemical properties

such as the cyclability of the cathode materials significantly compared with $LiFePO_4$ only powders.

Summary

Regardless of high capacity and stability during lithium extraction, $LiFePO_4$ materials have difficulty in applications such as high electrical density because of low electric conductivity. For the electrochemical study of this material, we synthesized $LiFePO_4$ powders and carbon coated $LiFePO_4$ powders by adding chitosan using the solid state reaction method. All powders were calcined in reduced argon atmosphere to avoid the oxidation of carbon. With the number of calcinations, we observed that Fe^{3+} is reduced to Fe^{2+} state from XPS study. We found that the carbon coating improved the cyclability of the cathode materials and the chitosan added $LiFePO_4$ increases the electrochemical performance for rechargeable batteries.

Acknowledgments. This work was supported by the grant No. RTI04-02-01 from the Regional Technology Innovation Program of the Ministry of Knowledge and Economy, Korea, and R01-2006-000-10742-0 from the Korean Science and Engineering Foundation, Korea.

References

1. Lee, T.; Cho, K.; Oh, J.; Shin, D. *J. Power Sources* **2007**, *174*, 394.
2. Yoon, W. S.; Chung, K. Y.; Balasubramanian, M.; Hanson, J.; McBreen, J.; Yang, X. Q. *J. Power Sources* **2006**, *163*, 234.
3. Zhao, M. S.; Song, X. P. *J. Power Sources* **2007**, *164*, 822.
4. Yang, J.; Xu, J. J. *J. Electrochem. Soc.* **2006**, *153*, A716.
5. Wang, G. X.; Needham, S.; Yao, J.; Wang, J. Z.; Liu, R. S.; Liu, H. K. *J. Power Sources* **2006**, *159*, 282.
6. Goodenough, J. B. *J. Power Sources* **2007**, *174*, 996.
7. Padhi, A. K.; Nanjandaswamy, K. S.; Goodenough, J. B. *J. Electrochem. Soc*. **1997**, *144*, 1188.
8. Kim, J. K.; Cheruvally, G.; Choi, J. W.; Kim, J. U.; Ahn, J. H.; Cho, G. B.; Kim, K. W.; Ahn, H. J. *J. Power Sources* **2007**, *166*, 211.
9. Zaghib, K.; Mauger, A.; Gendron, F.; Julien, C. M. *Solid State Ionics* **2008**, *179*, 16.
10. Padhi, A. K.; Nanjundaswamy, K. S.; Masquelier, C.; Okada, S.; Goodenough, J. B. *J. Electrochem. Soc*. **1997**, *144*, 1609.
11. Tarascon, J. M.; Armond, M. *Nature* **2001**, *414*, 359.
12. Chen, Z.; Dahn, J. R. *J. Electrochem. Soc*. **2002**, *149*, A1184.
13. Delacourt, C.; Wurm, C.; Laffont, L.; Leriche, J. B.; Masquelier, C. *Solid State Ionics* **2006**, *177*, 333.
14. Yamada, A.; Chung, S. C.; Hinokuma, K. *J. Electrochem. Soc*. **2001**, *148*, A224.
15. Andersson, A. S.; Thomas, J. O.; Kalska, B.; Haggstrom, L. *Electrochem. Solid-State Lett*. **2000**, *3*, 66.
16. Kim, C. W.; Park, J. S.; Lee, K. S. *J. Power Sources* **2006**, *163*, 144.
17. Sanchez, M. A. E.; Brito, G. E. S.; Fantini, M. C. A.; Goya, G. F.; Matos, J. R. *Solid State Ionics* **2006**, *177*, 497.
18. Nakamura, T.; Miwa, Y.; Tabuchi, M.; Yamada, Y. *J. Electrochem. Soc*. **2006**, *153*, A1108.
19. Salah, A. A.; Mauger, A.; Zaghib, K.; Goodenough, J. B.; Ravet, N.; Gauthier, M.; Gendron, F.; Julien, C. M. *J. Electrochem. Soc*. **2006**, *153*, A1692.
20. Wang, L. N.; Zhang, Z. G.; Zhang, K. L. *J. Power Sources* **2007**, *167*, 200.
21. Zane, D.; Carewska, M.; Scaccia, S.; Cardellini, F.; Prosini, P. P. *Electrochim. Acta* **2004**, *49*, 4259.
22. Jeong, E. D.; Kim, H. J.; Ahn, C. W.; Ha, M. G.; Hong, T. E.; Kim, H. G.; Jin, J. S.; Bae, J. S.; Hong, K. S.; Kim, Y. S.; Kim, H. J.; Doh, C. H.; Yang, H. S. *J. Nanosci. Nanotech*. **2009**, *9*, 4467.
23. Ahn, C. W.; Ha, M. G.; Hong, T. E.; Hong, K. S.; Jeong, E. D.; Kim, Y. S.; Doh, C. H.; Park, S.; Yang, H. S. *J. Nanoscience and Nanotechnology* (submitted).
24. Moulder, J. F.; Stickle, W. F.; Sobol, P. E.; Bomben, K. D. *Handbook of X-ray Photoelectron Spectroscopy*; Chastain, J.; King, R. C. Jr., Eds.; Physical Electronics, Inc: USA, 1995.
25. Myung, S. M.; Komaba, S.; Hirosaki, N.; Yashiro, H.; Kumagai, N. *Electrochimica Acta* **2004**, *49*, 4213.
26. Wu, X. M.; Li, X. H.; Xiao, Z. B.; Liu, J.; Yan, W. B.; Ma, M. Y. *Mater. Chem. Phys*. **2004**, *84*, 182.